

# Large Eddy Simulation of Turbulent Premixed Flame in Turbulent Channel Flow

**Sang Cheol Ko\***

*Department of Mechanical & Automotive Engineering, Jeonju University,  
Hyoja-dong 3 Ga 1200, Wansan-ku, Jeonju 560-759, Korea*

**Nam Seob Park**

*Research & Development Division for Hyundai & Kia Motor Company 772-1,  
Jangduk-Dong, Whasung-Si, Kyunggi-Do 445-706, Korea*

Large eddy simulation of turbulent premixed flame in turbulent channel flow is studied by using  $G$ -equation. A flamelet model for the premixed flame is combined with a dynamic subgrid combustion model for the filtered propagation flame speed. The objective of this work is to investigate the validity of the dynamic subgrid  $G$ -equation model to a complex turbulent premixed flame. The effect of model parameters of the dynamic subgrid  $G$ -equation on the turbulent flame speed is investigated. In order to consider quenching of laminar flames on the wall, wall-quenching damping function is employed in this calculation. In the present study, a constant density turbulent channel flow is used. The calculation results are evaluated by comparing with the DNS results of Bruneaux et al.

**Key Words :** Large Eddy Simulation (LES), Dynamic Subgrid Scale Model, Premixed Flame,  $G$ -Equation, Flame Front Propagation

## 1. Introduction

Turbulent premixed flames are important because of their occurrence in spark ignition engines and gas turbines in order to minimize  $\text{NO}_x$  formation. They are also subject of fundamental study to understanding of more complicated combustion phenomena as well as engineering concerns. Their behavior is difficult to describe since several interconnected processes – chemical reaction, diffusion, flame propagation, volume expansion – occur inhomogeneous flows. The challenges facing designs of combustion devices involve scale dependent unsteady dynamic behaviors that can-

not be simulated well with standard ensemble or time averaged flow model, and more accurate prediction method is required. Direct numerical simulation (DNS) of turbulent reacting flows are not practical since it demands extremely high computational resources. In large eddy simulation (LES), large scales are resolved whereas the effects of the smallest turbulent scales are modeled. In the field of combustion, the understanding and the control of combustion instabilities are domains where LES is required and will be applied in practical systems.

One of the practically relevant and better-understood types of turbulent premixed combustion is the laminar flamelet regime, in which the characteristic chemical time is much shorter than the characteristic flow time. Under this condition, combustion can be represented as the propagation of laminar flamelets, corrugated by turbulent eddies. In this study a flamelet model based on the  $G$ -equation is used (Kerstein et al., 1988). In a LES context, the  $G$ -equation is generally used to

---

\* Corresponding Author,

**E-mail :** scko@jj.ac.kr

**TEL :** +82-63-220-2623; **FAX :** +82-63-220-2056

Department of Mechanical & Automotive Engineering, Jeonju University, Hyoja-dong 3 Ga 1200, Wansan-ku, Jeonju 560-759, Korea. (Manuscript **Received** September 12, 2005; **Revised** May 15, 2006)

---

describe the filtered  $G$  field, where the propagation of the filtered flame front speed is modeled. Smith et al. (1994) proposed a subgrid model for combustion in LES using a  $G$  equation in which a subgrid scale turbulent flame speed is introduced. The turbulent flame speed is generally modeled extending experimental fits of the mean turbulent flame speed in Reynolds averaging context. Fundamental research is also carried out in this field by comparing different approaches with DNS results (Piana et al., 1996). Unfortunately, the turbulent flame speed is not well-defined quantity and the scatter of experimental data is very large. Then, no universal model is available for the subgrid scale turbulent flame speed. Recently, a dynamic subgrid model was proposed by Im et al. (1997) to overcome this difficulty. However, LES application using this dynamic subgrid model to a practical combustor not reported yet.

The interaction of a turbulent premixed flame with a wall is quite complex. The flame is strongly influenced by the presence of the wall that limits flame wrinkling and may cause the flame front to quench. Moreover, the flame has a significant effect on the flow in the vicinity of the wall: viscosity is greatly increased in the burnt gases, inhibiting turbulence. For these reasons, modeling flame wall interactions in turbulent flows is an important issue. However, little fundamental information is available so model building is difficult exercise. An additional problem is that experiments are difficult to perform because the interesting phenomena occur very close to wall.

The main objective of this work is to investigate the validity of the dynamic subgrid  $G$ -equation flamelet model to a turbulent premixed flame with wall. The effect of model parameters of the dynamic subgrid  $G$ -equation on the turbulent flame speed is investigated. A limitation of the  $G$ -equation approach is, however, that this model does not recognize walls and, therefore, some *ad hoc* models are usually required to prevent strange behavior near the walls. In order to consider quenching of laminar flames on walls, wall-quenching damping function is employed for the current LES. In the present study, a constant

density turbulent channel flow was used, and the predicted LES results are evaluated by comparing with the DNS results of Bruneaux et al. (1994).

## 2. Governing Equation

### 2.1 Some remarks on the $G$ -equation

It has been suggested that the propagating front may be captured by defining the front as a level contour of a continuous function of  $G$  (Kerstein et al., 1988).

$$\frac{\partial G}{\partial t} + u_j \frac{\partial_i G}{\partial x_j} = S_L |\nabla G| \quad (1)$$

In this equation, all information about the flame structure is carried by the flame speed  $S_L$ . This provides a convenient opening for large eddy simulation; the flame structure need not be modeled.

If one wishes to solve Eq. (1) in the constant-speed limit, i.e.,  $S_L = S_L^0$ , numerical difficulties arise due to the formation of cusps as the front propagates. Cusps are a natural consequence of constant-speed propagating fronts in much the same way as shocks are a characteristic feature of the Burgers equation; they are discontinuities in the derivatives of the solution and make numerical treatment very difficult. To overcome the numerical difficulties associated with cusps, previous studies introduced various types of diffusive terms (Kerstein et al., 1988). These terms are not entirely *ad hoc*, however; they can be shown to represent the effect of thermal relaxation under transverse heat diffusion in the preheat zone of a wrinkled front (Clavin, 1985). Using the asymptotic relation for  $S_L$ , Eq. (1) can be written as

$$\frac{\partial G}{\partial t} + u_j \frac{\partial_i G}{\partial x_j} = S_L^0 |\nabla G| + D \nabla^2 G \quad (2)$$

where only the leading term has been kept; this is a reasonable approximation provided the flame thickness is sufficiently small compared with the hydrodynamic scale. In the above relation,  $D = S_L^0 L$  is the Markstein diffusivity, where the Markstein length,  $L$  is typically normalized by the flame thickness  $l_f$ . Since

$$l_f = \frac{\alpha}{S_L^0} = \left( \frac{1}{S_L^0} \right) \left( \frac{\nu}{Pr} \right) \quad (3)$$

Therefore,

$$D = \left( \frac{\nu}{\text{Pr}} \right) Ma \quad (4)$$

where  $\alpha$  and  $\nu$  are the thermal diffusivity and kinematic viscosity, Pr the Prandtl number and  $Ma = L/l_f$  the Markstein number, which is ideally a property of the mixture (Clavin et al., 1979) and typically of  $O(1)$  quantity in practical flame.

## 2.2 Basic equations

The flow solves the Navier–Stokes equations for an incompressible, constant viscosity flow :

$$\frac{\partial \tilde{\rho} \tilde{u}_i}{\partial \tilde{t}} + \frac{\partial (\tilde{\rho} \tilde{u}_j \tilde{u}_i)}{\partial \tilde{x}_j} = - \frac{\partial \tilde{p}}{\partial \tilde{x}_i} + \mu \frac{\partial^2 \tilde{u}_i}{\partial \tilde{x}_j^2} \quad (5)$$

$$\frac{\partial \tilde{u}_i}{\partial \tilde{x}_i} = 0 \quad (6)$$

The reaction solves the energy conservation equation and  $G$ -equation, which allows convection, diffusion, and reaction effects :

$$\begin{aligned} & \frac{\partial \tilde{\rho} c_p \tilde{T}}{\partial \tilde{t}} + \frac{\partial \tilde{\rho} C_p \tilde{u}_i \tilde{T}}{\partial \tilde{x}_i} \\ &= - \frac{\partial}{\partial \tilde{x}_i} \left( \lambda \frac{\partial \tilde{T}}{\partial \tilde{x}_i} \right) + C_p (\tilde{T}_2 - \tilde{T}_1) \tilde{\omega}_R \end{aligned} \quad (7)$$

$$\frac{\partial \tilde{\rho} G}{\partial \tilde{t}} + \frac{\partial \tilde{\rho} \tilde{u}_i G}{\partial \tilde{x}_i} = \tilde{\rho} \tilde{S}_L^0 |\nabla G| + D \nabla^2 \tilde{\rho} G \quad (8)$$

The superscript ( $\sim$ ) refers to physical variables ; absence of superscript indicates a dimensionless variable.

We assume  $\lambda = \lambda_i \lambda^*$  where  $\lambda^* = (\tilde{T}/\tilde{T}_1)$ . The subscript 1 refers to the fresh gases, and the subscript 2 refers to the burnt gases. In the flow field, the value of  $G$  is prescribed in the range  $[0, 1]$ . Here,  $G$  is assigned the value of zero in the unburned region and unit in the burnt region with the thin flame identified by a fixed value of  $0 < G_0 < 1$ . The  $G$ -equation (8) must be solved along with the Eqs. (7) and (8) since  $G$  is coupled with the heat release term of energy conservation Eq. (7) (Piana et al., 1996) :

$$\tilde{\omega}_R = \tilde{\rho} \tilde{S}_L^0 |\nabla G| \quad (9)$$

The equations are non-dimensionalized using the

following dimensional quantities :  $\tilde{u}_\tau^0$  the friction velocity at the wall,  $\tilde{h}$  the channel half width,  $\tilde{T}_1$  the temperature in the fresh gases,  $\tilde{T}_2$  the temperature in the hot gases. Physical and dimensionless variable are related in the following way :

$$\begin{aligned} \tilde{u} &= \tilde{u}_\tau^0 u, & \tilde{t} &= \tilde{h} t / \tilde{u}_\tau^0, & \tilde{p} &= \tilde{\rho} \tilde{u}_\tau^0{}^2 \rho \\ \tilde{x} &= \tilde{h} x, & T &= (\tilde{T} - \tilde{T}_1) / (\tilde{T}_2 - \tilde{T}_1) \end{aligned}$$

The filtering operation resulting equations with non-dimensionalized can be written as :

$$\begin{aligned} & \frac{\partial \bar{u}_i}{\partial t} + \frac{\partial (\bar{u}_i \bar{u}_j)}{\partial x_j} \\ &= - \frac{\partial \bar{p}}{\partial x_i} + \frac{\partial}{\partial x_j} \frac{1}{\text{Re}} \left( \frac{\partial \bar{u}_i}{\partial x_j} + \frac{\partial \bar{u}_j}{\partial x_i} \right) - \frac{\partial \tau_{ij}^{sgs}}{\partial x_j} \end{aligned} \quad (10)$$

$$\frac{\partial \bar{u}_i}{\partial x_i} = 0 \quad (11)$$

$$\frac{\partial \bar{T}}{\partial t} + \frac{\partial (\bar{T} \bar{u}_j)}{\partial x_j} = \frac{\partial}{\partial x_j} \left( \frac{\lambda^*}{\text{RePr}} \frac{\partial \bar{T}}{\partial x_j} \right) - \frac{\partial q_j^{sgs}}{\partial x_j} + \dot{\omega} \quad (12)$$

$$\dot{\omega} = S_L^0 |\nabla G| \quad (13)$$

$$\frac{\partial \bar{G}}{\partial t} + \frac{\partial (\bar{G} \bar{u}_j)}{\partial x_j} = S_L^0 |\nabla G| - \frac{\partial \gamma_j^{sgs}}{\partial x_j} + D \frac{\partial^2 \bar{G}}{\partial x_j^2} \quad (14)$$

where the Reynolds numbers is  $\text{Re} = \tilde{\rho} \tilde{u}_\tau^0 \tilde{h} / \mu$ , the Prandtl numbers is  $\text{Pr} = \mu C_p / \lambda_i$ .

Here the unclosed subgrid terms representing respectively, the subgrid tensor  $\tau_{ij}^{sgs}$ , the subgrid heat flux  $q_j^{sgs}$  are need to be modeled.

$$\tau_{ij}^{sgs} = \overline{u_i u_j} - \bar{u}_i \bar{u}_j \quad (15)$$

$$q_j^{sgs} = \overline{u_j T} - \bar{u}_j \bar{T} \quad (16)$$

In the  $G$ -equation (14), both the subgrid scalar flux,  $\gamma_j^{sgs}$ , and the filtered modulus term,  $|\nabla G|$  must be modeled.

$$\gamma_j^{sgs} = \overline{u_j G} - \bar{u}_j \bar{G} \quad (17)$$

## 2.3 Dynamic subgrid scale model for $G$ -equation

In this study, the subgrid flux terms in Eq. (14) is modeled by an eddy diffusivity model analogous to Smagorinsky model, i.e., (Im et al., 1997),

$$\gamma_k^{sgs} = \overline{u_k G} - \bar{u}_k \bar{G} = -\alpha_t \frac{\partial \bar{G}}{\partial x_k}, \quad \alpha_t = C_0 \Delta^2 |\bar{S}| \quad (18)$$

Similarly, at the test filter level,

$$\Gamma_k = \overline{u_k \widehat{G}} - \widehat{u}_k \widehat{G} = -\widehat{\hat{a}}_t \frac{\partial \widehat{G}}{\partial x_k}, \quad \widehat{\hat{a}}_t = C_G \widehat{\Delta}^2 |\widehat{S}| \quad (19)$$

A generalization of Germano's identity (1991) can be used to determine the constant  $C_G$ .

$$F_k^G = \Gamma_k = -\widehat{\hat{\gamma}}_k^{sgs} = \overline{u_k \widehat{G}} - \widehat{u}_k \widehat{G} \quad (20)$$

Using Eqs. (18) ~ (20) with the least-squares method (Lilly, 1992), we can obtain

$$C_G \Delta^2 = -\langle F_i^G H_i^G \rangle / \langle H_j^G H_j^G \rangle \quad (21)$$

where

$$H_k^G = (\widehat{\Delta} / \Delta)^2 |\widehat{S}| \frac{\partial \widehat{G}}{\partial x_k} - |\widehat{S}| \frac{\partial \overline{G}}{\partial x_k} \quad (22)$$

Here  $\overline{S}_{ij}$  is the strain rate,  $\overline{\Delta}$  is the grid filtered characteristic length scale and  $\widehat{\Delta}$  is the test filter width.

$$|\widehat{S}| = (2\overline{S}_{ij}\overline{S}_{ij})^{1/2}, \quad \overline{S}_{ij} = \frac{1}{2} \left( \frac{\partial \overline{u}_i}{\partial x_j} + \frac{\partial \overline{u}_j}{\partial x_i} \right) \quad (23)$$

The propagation term for filtered  $G$ -equation is approximated as,

$$S_L^G |\nabla G| = \overline{S}_T |\nabla \overline{G}| \quad (24)$$

where  $\overline{S}_T$  is the filtered turbulent flame front speed averaged over a characteristic LES cell and must be modeled.

The LES subgrid scale combustion model for turbulent flame speed can be obtained by using dynamic processes induced by Im et al. (1997). The resulting formulation can be written as:

$$\frac{\overline{S}_T}{S_L^0} = 1 + C_{GPD} \left( \frac{q}{S_L^0} \right)^n \quad (25)$$

$$C_{GPD} = \frac{(S_L^0)^n \left[ \langle |\widehat{\nabla G}| \rangle - \langle |\nabla \widehat{G}| \rangle \right]}{\left[ \langle Q^n |\nabla \widehat{G}| \rangle - \langle q^n |\widehat{\nabla G}| \rangle \right]} \quad (26)$$

where the brackets denotes a volume averaged. Here,  $n$  is a constant,  $q$  is the rms of the subgrid turbulent intensity, and  $Q$  is the rms of the test-grid scale turbulent intensity.

In this study, the subgrid kinetic energies are modeled by using the Im's model similar to that of Bardina et al. (1980),

$$q^2 = \overline{\overline{u}_i \overline{u}_i} - \overline{\overline{u}_i} \overline{\overline{u}_i} \quad (27)$$

where the "double-bar" denotes applying the same filter twice.

Similarly, at the test-filter level one can estimate the unresolved kinetic energy,  $Q^2$ , as the difference between the test-filtered, and the twice-test-filtered field,

$$Q^2 = \widehat{\widehat{u}_i \widehat{u}_i} - \widehat{\widehat{\widehat{u}_i \widehat{u}_i}} \quad (28)$$

### 3. Numerical Method

In this study, three-dimensional LES channel flow code is extended to a turbulent premixed combustion flow, to take reaction into account. Temperature and  $G$ -field are treated as scalars and do not affect the flow. The subgrid scale models for scalar transportations are introduced.

The governing equations are discretized on a staggered mesh by finite volume technique. Second order schemes are used in space and time, central differencing for convection and diffusion terms and Adams-Bashforth schemes in time. A time marching procedure to a couple velocity-pressure is performed by SMAC method. The dimension of the computational domains are  $2\pi h$ ,  $2h$  and  $\pi h$  (where  $h$  is the channel half-height) with a grid of  $32 \times 64 \times 32$ , respectively, in the  $x$ ,  $y$ , and  $z$  directions (Fig.1). The smallest grid resolution normal to the wall set to  $y^+ = 1$  (giving a streamwise resolution of  $\Delta x^+ = 70.7$  and spanwise resolution of  $\Delta z^+ = 23.5$  in wall units, respectively). Reynolds number normalized by the channel half-height and wall friction velocity was set to  $Re_x = 180$  ( $u_\tau h / \nu$ ).

The walls are no-slip and isothermal. The flow, temperature and  $G$ -scalar fields are periodic in  $x$  and  $z$  directions. The main flow was sustained by explicitly adding the pressure gradient for the streamwise direction.

The initial conditions for the flow are obtained

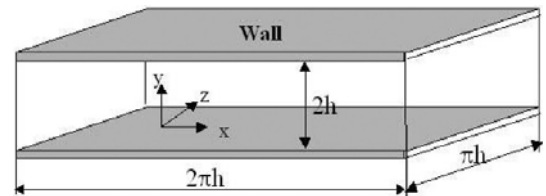


**Fig. 1** Schematic diagram of the computational domain

by running the flow solver until stabilized values of the velocities and pressure are obtained. The initial values of temperature and  $G$ -scalar are imposed at the center of channel as one-dimensional laminar flames propagating towards the walls.

### 4. Results and Discussion

LES of turbulent premixed flames are performed to validate dynamic subgrid combustion model in turbulent channel flow. Calculation parameters for LES of turbulent premixed flame were specified as shown in Table 1. In this study, the Markstein diffusivity  $D$  is set as  $D=4\nu_t$ , where  $\nu_t=C\Delta^2|\bar{S}|$  (Im et al., 1997). In order to consider quenching of laminar flames on walls, wall-quenching damping function  $f_Q$  is introduced and  $f_Q$  is multiplied to the laminar flame speed.

$$f_Q=[1+\exp\{-0.5(y^+-y_Q^+)\}]^{-1}$$

Here,  $y^+$  is a wall unit and  $y_Q^+$  is a quenching distance. In this study,  $y_Q^+$  is assigned as 28, which was referred from DNS results of  $G$ . Bruneaux et al. (1994).

Initial conditions for temperature and  $G$ -field distributions are given as to 1.0 at the  $x-z$  plane

**Table 1** Fixed parameters for LES of turbulent premixed flame

Re	Pr	Le	$S_L^0/u_\tau$	$d/h$	$\bar{T}_2/\bar{T}_1$
180	0.5	1	0.363	0.03	4

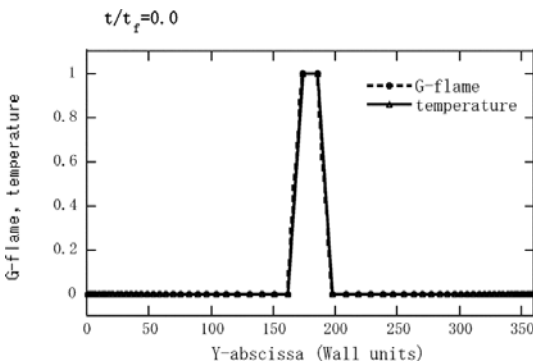


**Fig. 2** Initial conditions of the temperature and  $G$ -field distribution

of the half-height channel and other regions equal to 0.0 as shown in Fig. 2.

Numerical simulations are performed for three cases, which are summarized in Table 2, to investigate the effect of model parameters of the dynamic subgrid  $G$ -equation on the turbulent flame speed.

Figure 3 shows profiles of the square roots of the subgrid kinetic energy associated with the grid-filtered and test-filtered volume, respectively,  $q$  and  $Q$ . Figure 4 shows the evolution of the

**Table 2** Case specification

	Markstein diffusivity	exponent $n$
Case 1	yes	1
Case 2	no	1
Case 3	yes	2

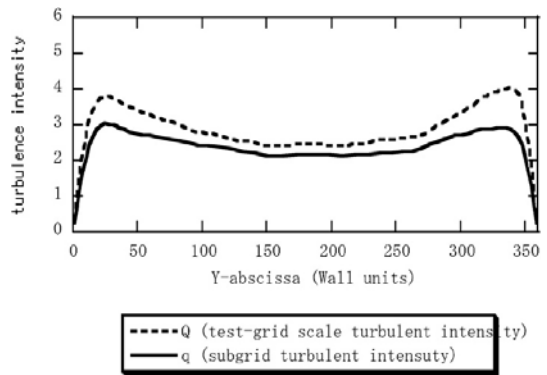


**Fig. 3** Profiles of the subgrid scale turbulence intensity  $q$  and the test filtered scale turbulence intensity  $Q$

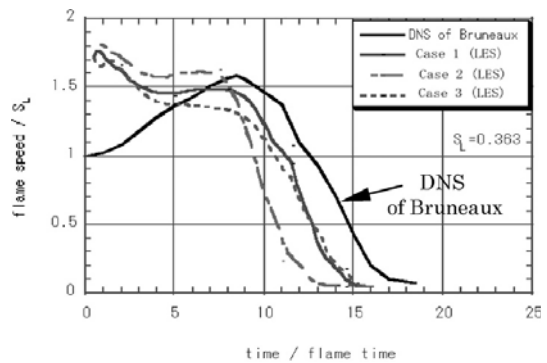


**Fig. 4** Evolution of normalized turbulent flame speed during flame wall interaction

turbulent flame speed normalized by the undistributed laminar flame speed  $S_L^0=0.363$ . The reason for the difference of flame speed in early times between DNS and LES results are caused by the initial conditions of calculation. In LES, the SGS model for the flame front propagation speed is applied. On the other hand, the DNS results are solved the equation based on the reaction rate so that the flame speed is increased along with temperature in early times.

In case 1, the turbulent flame speed is somewhat large at early time, producing a maximum turbulent speed 1.7 times of the laminar flame speed, but it has no physical meaning, in spite of weak turbulence near the center of the channel. This overestimation of the turbulent speed at early time is caused that the  $G$ -field is given by a discontinuous distribution initially so that the gradient of  $G$  is very large. In case 1, until  $t/t_f < 3$  where  $t_f=d/S_L=\lambda_i/\rho C_p(S_L^0)^2$ ,  $d$  is a typical flame thickness and  $S_L^0$  the undistributed laminar flame speed, the turbulent flame speed decreases as does the gradient of  $G$ . After  $t/t_f > 3$ , the turbulent flame speed remains constant a turbulent speed 1.45 times of the laminar flame speed for a while (about 3.5 to 5.5 flame times) ; then, the turbulent flame speed increases as does sub-grid turbulent intensity and reaches a plateau (near the turbulent flame speed 1.5 times of the laminar flame speed) before the flame begins to interact with the wall quenching until  $t/t_f=8.5$  and, finally it is reduced by interaction with the wall. For the case 2, which was not applied with the Markstein diffusivity, the predicted turbulent flame speed is about 10% larger than compared with that of case 1 at early times, but the slope of wall quenching effect is a little more steep. However, the general behavior of the flame is the same with case 1. For the case 3, predicted turbulent flame speed applied with an exponent  $n=2$  is about 8% smaller than that of case 1 applied with  $n=1$ .

Figure 5 presents the iso-surface of temperature  $T=0.85$  in the turbulent flame at  $t/t_f=6.05$ . At this time flame passed through  $y^+=90$  wall distance, for case 1.

Mean values of  $G$  distribution, temperature,

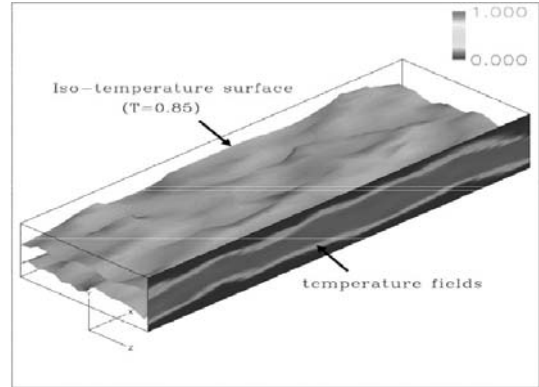
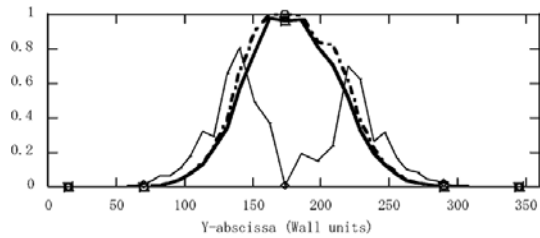
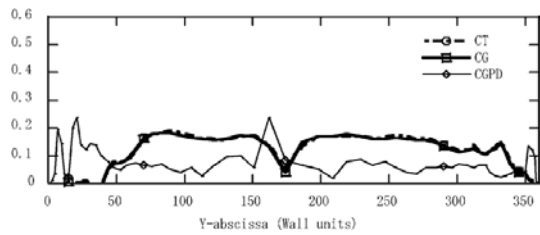


Fig. 5 Snapshot of iso-surface of temperature ( $T=0.85$ ) at  $t/t_f=6.05$ , at this time flame passed through  $y^+=90$  wall distance. (Case 1)



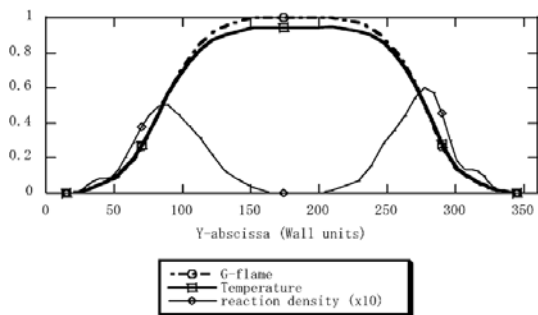
(a)



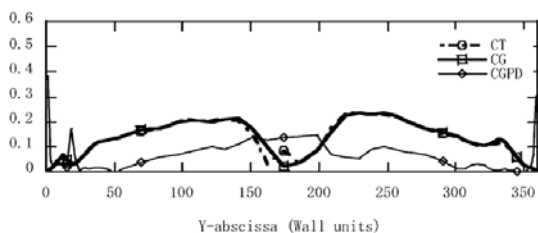
(b)

Fig. 6 Mean values of flame propagation properties at  $t/t_f=1.8$  (Case 1) (a) Profiles of  $G$ , temperature and equivalent reactive flame surface density. (b) Profiles of model constants by dynamic SGS model

reaction rate and model constants,  $C_T$ ,  $C_G$  and  $C_{GPD}$ , obtained by LES for case 1 are shown in Figs. (6) ~ (8), respectively, at flame times  $t/t_f=1.8, 6.05$  and  $12.7$ . The profiles of  $G$ -flame and temperatures are propagated towards the walls in times. In this calculation, the reaching time of initial flame to the wall quenching distance



(a)



(b)

**Fig. 7** Mean values of flame propagation properties at  $t/t_f=6.05$ ,  $G=0.5$  —iso—surface passed  $y^+=90$  wall distance (Case 1) (a) Profiles of  $G$ , temperature and equivalent reactive flame surface density. (b) Profiles of model constants by dynamic SGS model

( $y_q^+=28$ ) is  $t/t_f=12.7$ , which is reproduced well compared with the DNS results of  $t/t_f=12.8$  (Bruneaux et al.,1996).

## 5. Conclusions

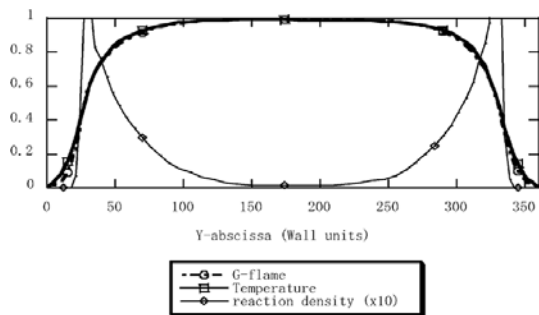
Large eddy simulation of turbulent premixed flame in turbulent channel flows are performed by using dynamic subgrid combustion model. The effects of the model parameters were investigated in three types of LES calculations. The conclusions are as follows :

- (1) The effect of the Markstein diffusivity

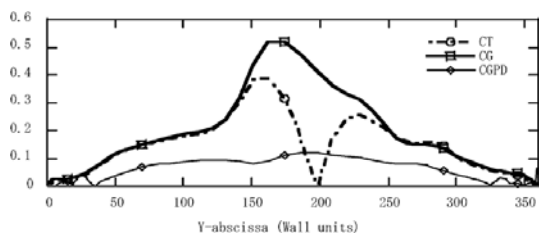
The Markstein diffusivity makes the turbulent flame speed a small because the gradient of  $G$ ,  $|\nabla G|$ , was decreased by the Markstein diffusion. In this study, predicted turbulent flame speed with the Markstein diffusivity is about 10% smaller than that of without concerned it.

- (2) The effect of the exponent  $n$

Predicted turbulent flame speed applied with



(a)



(b)

**Fig. 8** Mean values of flame propagation properties at  $t/t_f=12.7$ ,  $G=0.5$  —iso—surface passed  $y^+=28$  wall distance (Case 1) (a) Profiles of  $G$ , temperature and equivalent reactive flame surface density. (b) Profiles of model constants by dynamic SGS model

an exponent  $n=2$  is about 8% smaller than that of applied with  $n=1$ . In this study, the simulation result with  $n=1$  shows better agreement with the DNS results.

(3) The predicted turbulent flame velocity adopted with dynamic subgrid  $G$ -equation model is strongly dependent on initial condition of  $G$ -field distribution. In this LES calculation, the rapid gradient of initial conditions of  $G$ -field distribution lead to excessive turbulent flame velocity in early times. However, after flames diffused well with turbulence, the predicted turbulent flame velocities shows reasonable that the values are 1.5 times of laminar flame speed which is closed to the DNS result of Bruneaux et al..

## References

- Bardina, J., Ferziger, J. H. and Reynolds, W. C., 1980, "Improved Subgrid-Scale Models for Large Eddy Simulation," *AIAA Paper* No. 80-

1357.

Bruneaux, G., Akselvoll, K., Poinso, T. J. and Ferziger, J. H., 1994, "Simulation of a Turbulent Flame in a Channel," *Center for Turbulent Research Proc. of the Summer Program*, Stanford University, pp. 157~174.

Clavin, P., 1985, "Dynamic Behavior of Premixed Flame Fronts in Laminar and Turbulent Flow," *Prog. Energy Combust. Sci.*, 11, pp. 1~59.

Clavin, P. and Williams, F. A., 1979, "Theory of Premixed-Flame Propagation in Large-Scale Turbulence," *J. Fluid Mech.*, 90, pp. 589~604.

Germano, M., Piomelli, U., Moin, P. and Cabot, W. H., 1991, "A Dynamic Subgrid-Scale Eddy Viscosity Model," *Phys. Fluids A*, 3, pp. 1760~1765.

Im, H. G. and Lund, T. S., 1997, "Large Eddy Simulation of Turbulent Front Propagation with Dynamic Subgrid Models," *Phys. Fluids*, 9 (12),

pp. 3826~3833.

Kerstein, A. R., Ashurst, Wm. T. and Williams, F. A., 1988, "Field Equation for Interface Propagation in an Unsteady Homogenous Flow Field," *Phys. Rev. A*, Vol. 37, No. 7, pp. 2728~2731.

Lilly, D. K., 1992, "A Proposed Modification of the Germano Subgrid-Scale Closure Method," *Phys. Fluids A*, 4, pp. 633~635.

Piana, J., Veynante, D., Candel, S. and Poinso, T., 1996, "Direct Numerical Simulation Analysis of the G-Equation in Premixed Combustion," *Proc. 2<sup>nd</sup> ERCOFTAC Workshop on Direct and Large Eddy Simulation, Grenoble, France*, pp. H.4.1~4.10.

Smith, T. M. and Menon, S., 1994, "The Structure of Constant-Property Propagating Surfaces in a Spatially Evolving Turbulent Flow," *25<sup>th</sup> AIAA Fluid Dynamic Conferences*, pp. 1~13.